

Enantiomerically Enriched Aziridine-2-carboxylates via Copper-Catalyzed Reductive Kinetic Resolution of 2*H*-Azirines

Yinuo Zheng, Elvis Wang Hei Ng, Antonio Rizzo,* and Pauline Chiu*

Abstract: We present the first reductive kinetic resolution of racemic 2*H*-azirines to prepare optically enriched *N*-H aziridine-2-carboxylates, which are bench stable and readily diversifiable building blocks, concomitantly with the corresponding enantiomerically enriched 2*H*-azirines. The *N*-H aziridines were obtained with excellent diastereoselectivity (>20:1) and high enantioselectivity (up to 94%). A Hammett study revealed a linear free energy relationship between the $\Delta\Delta G^\ddagger$ of the diastereomeric transition states and the σ_p^- values. Density functional theory (DFT) calculations and non-covalent interaction analysis suggested that non-classical H-bonding interactions and edge-to-face aromatic interactions between the substrate and the ligand are responsible for the stereoselectivity and also for the substrate electronic effects observed in the Hammett study.

Introduction

Aziridine-2-carboxylate esters are versatile chiral building blocks with a potential for many synthetic elaborations. For example, the aziridine moiety can undergo stereoselective ring openings and 1,3-dipolar cycloadditions; the ester functional group can also be manipulated (Scheme 1a).^[1–4] The

utility of this building block is well-demonstrated by its extensive application in the synthesis of bioactive molecules (Scheme 1b). For example, aspartic acid protease inhibitor aziridine dipeptide (I) has been prepared by amidation of the corresponding racemic aziridine-2-carboxylate with enantiomerically pure amino acids, followed by separation of the diastereomers.^[5,6] The hydantoin skeleton of BIRT-377 (II), a compound developed for the treatment of inflammatory and immune disorders, has been synthesized by reductive ring opening of the corresponding optically enriched 3-arylaziridine-2-carboxylate.^[7] Antibiotics featuring vicinal stereocenters, like (+)-chloramphenicol (III),^[8] (+)-thiamphenicol (IV)^[9] and florfenicol (V),^[10] as well as pro-drugs like L-DOPA (VI)^[11] and droxidopa (VII),^[12] have been prepared by regio- and stereoselective nucleophilic ring opening of enantiomerically pure aziridines. The aziridine moiety also served as the azomethine ylide precursor for the intramolecular 1,3-dipolar cycloaddition in a synthesis of a neurokinin (NK)-1 receptor (VIII).^[4] The first total synthesis of the potent antimicrobial agent dynobactin A (IX) in 2024 by Baran and coworkers showcased the utility of free *N*-H aziridines (e.g., *cis*-2*v*, 87% ee) as key building blocks via stereo- and regioselective C–C (western fragment) and N–C (eastern fragment) ring opening transformations.^[13]

Traditional strategies for the asymmetric synthesis of aziridine-2-carboxylates include intramolecular substitution of chiral amino esters,^[14–20] asymmetric aziridination of imines mediated by chiral ruthenium^[21] or borate catalysts,^[7,22–25] and asymmetric aziridination of alkenes via chiral copper catalysis (Scheme 2a).^[29] However, most of the reported procedures deliver aziridines bearing electron-deficient *N*-protecting groups, such as *N*-sulfinyl,^[14] *N*-sulfonyl,^[20,29] *N*-phosphonyl,^[16] and *N*-carbamoyl groups.^[17,19] Indeed, such *N*-deprotections can be non-trivial, as these activated aziridines are less stable and can undergo undesired ring opening.^[13] On the other hand, chiral *N*-H aziridines are more versatile building blocks, as they are generally bench stable under most circumstances for extended periods of time.^[1] Moreover, should their ring-opening reactivity be desired, they can be *N*-functionalized at the later stages of a synthetic route.

A straightforward preparation of enantiomerically enriched aziridine-2-carboxylates is conceivable through asymmetric nucleophilic additions to 2*H*-azirine derivatives.^[30–41] In this connection, the kinetic resolution (KR) of racemic 2,3-disubstituted 2*H*-azirines has emerged as a useful strategy to access optically enriched *N*-H aziridines and 2*H*-azirines (Scheme 2b). While highly enabling, only five

[*] Y. Zheng, Dr. A. Rizzo, Prof. Dr. P. Chiu

Department of Chemistry, and State Key Laboratory of Synthetic Chemistry, The University of Hong Kong, Pokfulam Road, Hong Kong, P.R. China

E-mail: anrich@hku.hk


pchiu@hku.hk


Dr. E. W. H. Ng

Department of Pharmacology and Pharmacy, LKS Faculty of Medicine, The University of Hong Kong, Pokfulam Road, Hong Kong, P.R. China

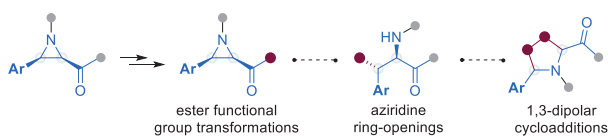
Prof. Dr. P. Chiu

Laboratory for Synthetic Chemistry and Chemical Biology Limited, Hong Kong Science Park, Shatin, Hong Kong

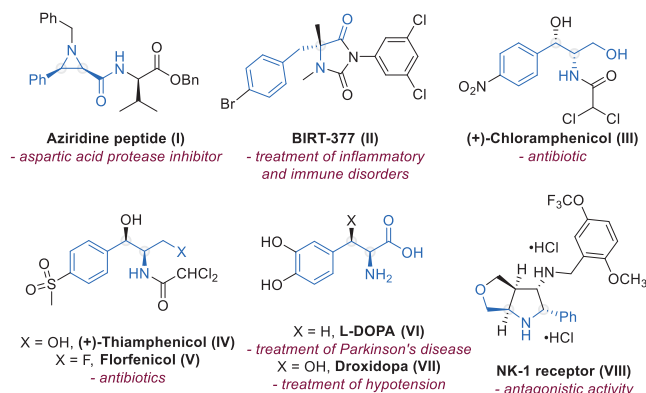
 Additional supporting information can be found online in the Supporting Information section

 © 2025 The Author(s). Angewandte Chemie International Edition published by Wiley-VCH GmbH. This is an open access article under the terms of the [Creative Commons Attribution-NonCommercial-NoDerivs](https://creativecommons.org/licenses/by-nc-nd/4.0/) License, which permits use and distribution in any medium, provided the original work is properly cited, the use is non-commercial and no modifications or adaptations are made.

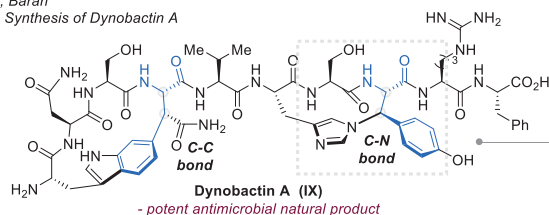
a) Synthetic potential of aziridine-2-carboxylates



b) 3-Arylaziridine-2-carboxylates used in the syntheses of bioactive molecules



2024, Baran
Total Synthesis of Dynobactin A

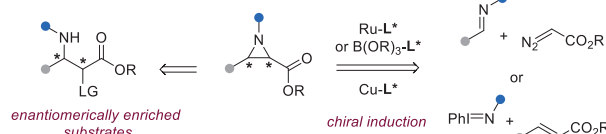
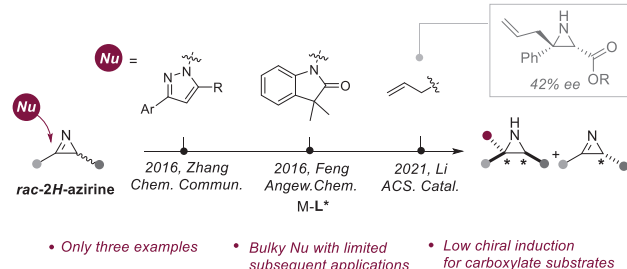


Scheme 1. a) Chiral aziridine-2-carboxylates can be leveraged as building blocks through S_N2 ring opening, ester group transformations, and as chiral 1,3-dipole precursors. b) Reported bioactive molecules that were synthesized using aziridine-2-carboxylates as starting materials.

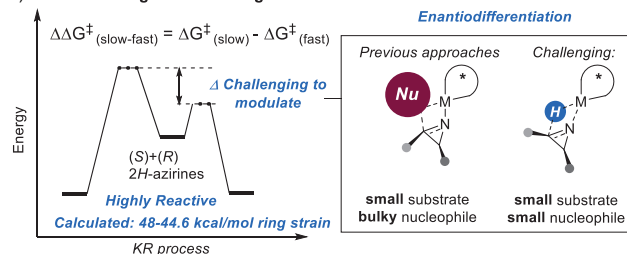
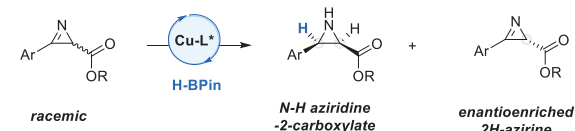
examples of 2*H*-azirine *KR* have been reported.^[30,31,33,38,40] Indeed, excellent ee's (up to 99%) have been achieved in these processes, but the incorporation of rather specific and exotic nucleophiles severely limits the application of these protocols to general syntheses. Recently, Li and coworkers were able to prepare more versatile 3-allylated aziridine-2-carboxylates, but with low chiral induction (42% ee).^[38]

Inspired by these reports and as part of our research program on copper hydride reduction chemistry,^[42–50] we speculated that chiral copper hydrides could be leveraged to differentiate the enantiomers of racemic 2*H*-azirine-2-carboxylates to access more synthetically relevant, optically enriched *N*-H-aziridine-2-carboxylates (Scheme 2c). We recognize that copper-catalyzed kinetic resolutions have been applied to substrates whose reactivities are attenuated, therefore facilitating their enantio-discrimination.^[51–53] On the other hand, 2*H*-azirine-2-carboxylates are highly reactive,^[54] with a calculated total ring strain of 44.6–48 kcal mol^{−1}.^[26–28] Moreover, hydrides are small nucleophiles in comparison

a) Methods to access enantiomerically enriched aziridine-2-carboxylates

b) The state-of-the-art for kinetic resolutions of 2*H*-azirines

c) Reaction design and challenges

d) This work: reductive kinetic resolution of 2*H*-azirine-2-carboxylates

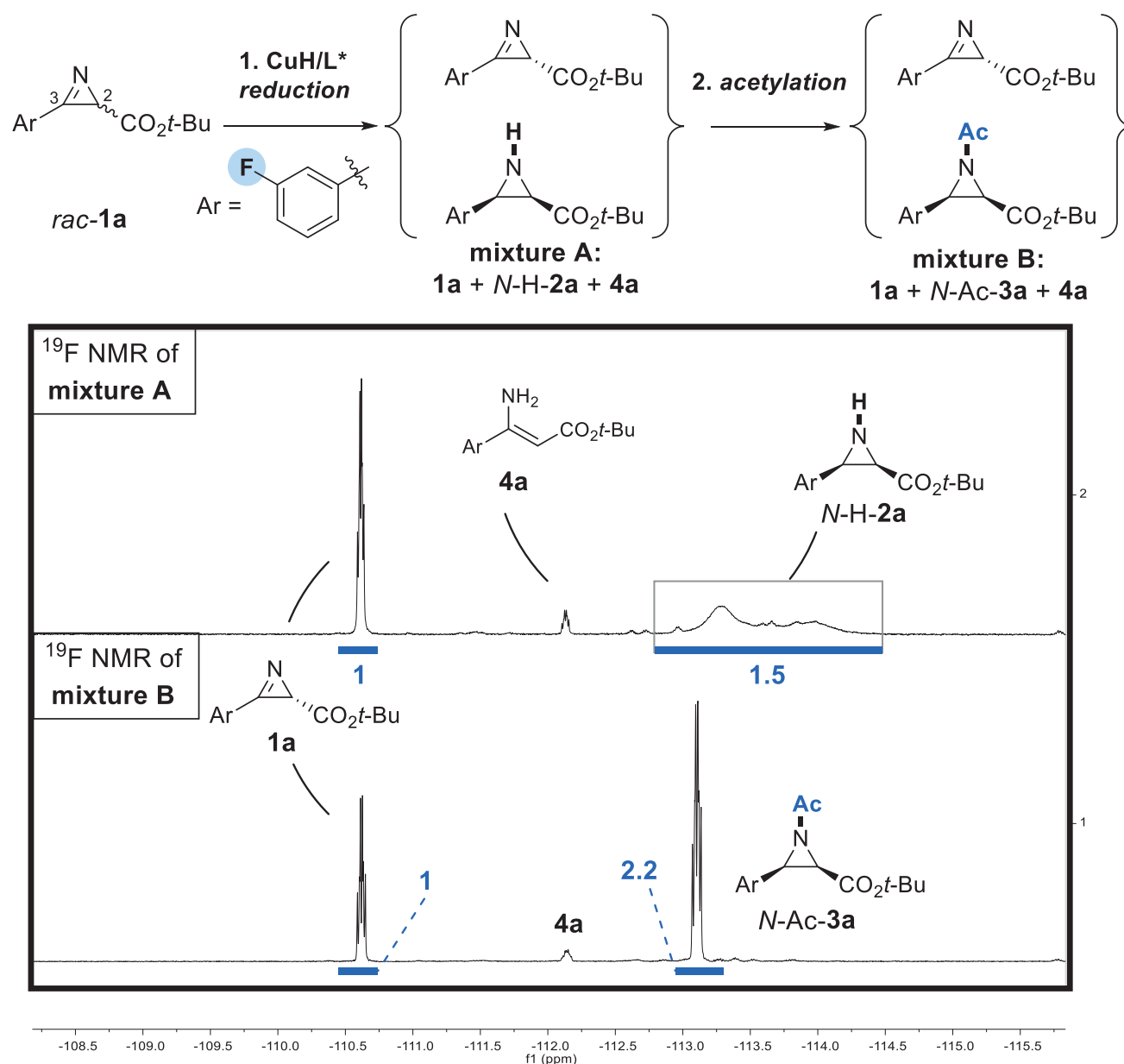
- First CuH-catalyzed asymmetric reduction of azirines
- Up to 94% ee
- Valuable products and broad synthetic applications
- Mechanistic study

Scheme 2. a) Reported strategies for the synthesis of chiral aziridine-2-carboxylates. b) Reported *KR* of 2*H*-azirines with their corresponding nucleophiles. c) Representation of the challenges of a reductive *KR* of 2*H*-azirines with hydride as the nucleophile and the calculated total ring strain of 2*H*-azirine.^[26–28] d) Highlights of this work.

to those used in the previous successful examples of *KR*, making the enantio-discrimination all the more challenging. Herein, we describe the realization of this reductive process to access various enantiomerically enriched 2*H*-aziridine-2-carboxylates. To the best of our knowledge, there has only been one communication of an asymmetric reduction of prochiral 2*H*-azirines, which reported low levels of chiral induction.^[55] Therefore, this report also represents the first asymmetric reduction to produce aziridines with good ee's (Scheme 2d).

Results and Discussion

To facilitate our study of the kinetic resolution process, we designed an experimental protocol that could efficiently



Scheme 3. Reaction optimization workflow for reductive KR by ¹⁹F NMR spectroscopy and acetylation to obtain accurate **1a:3a** ratios by integration.

evaluate the crude reaction mixtures without chromatographic purification of each run. We selected fluorinated 2H-azirine-2-carboxylate racemate (**1a**) as the model substrate to exploit ¹⁹F NMR to analyze the crude reaction mixtures (Scheme 3). Nevertheless, the free “N-H” of the aziridine product **2a** has a negative effect on both ¹H and ¹⁹F NMR analysis, so that, depending on the acid content of the deuterated solvent, the observed chemical shifts of **2a** vary (mixture A). Thus, for analytical purposes, we acetylated the crude product after the copper hydride catalyzed reduction. This enabled distinct and informative ¹⁹F NMR spectral analysis of the crude material **3a** (mixture B). Indeed, the apparent ratio of **1a:2a** versus **1a:3a** by integration before and after acetylation differs, therefore underscoring the necessity of N-protection for accurate analysis of the crude reduction

product. In the reduction, we also observed variable amounts of a side product, **4a**, which arises from hydride ring opening at the C-2 position of **1a**.

After an initial screening, CuTC (copper(I) thiophene-2-carboxylate) was selected as the copper source, as it provided the most reliable and consistent rates of in situ Cu–H formation (see Section 4.1 in the Supporting Information). Moreover, we found that at low catalyst loadings, oxygen exclusion was necessary to ensure the stability of the copper hydride. In the presence of CuTC (1 mol%), (*R*)-BINAP (**L1**) (1.2 mol%) and TMDS (0.5 equiv.) in THF (0.2 M with respect to **1a**) at room temperature for 18 h, the kinetic resolution of racemic-**1a** followed by acetylation successfully afforded aziridine *cis*-**3a** with >20:1 dr and 60% ee, together with recovered **1a** (Table 1, **L1**). As previously reported, the high

Table 1: Selected results from chiral ligand screening.^{a)}

Chiral ligand screening	
<p>L1: (R)-BINAP 1a 44% yield, 52% ee cis-3a 45% yield, 60% ee s = 7</p>	<p>L2: (R)-DTBM-SEGPHOS 1a 89% yield, 4% ee cis-3a 4% yield, 17% ee s = 1 (Ar = 3,5-(t-Bu)-4-MeO-C₆H₃)</p>
<p>L3: (R)-Difluorophos 1a 87% yield, 8% ee cis-3a 10% yield, 76% ee s = 8</p>	
<p>L4: (R, Sp)-Josiphos 1a 53% yield, 15% ee cis-3a 32% yield, 37% ee s = 3</p>	<p>L5: (R)-QuinoxP 1a 57% yield, 21% ee cis-3a 32% yield, 39% ee s = 3</p>
<p>L6: (R)-SDP n.r.</p>	
<p>L7: (R,R)-Me-DuPhos 1a 87% yield, 2% ee cis-3a 2% yield, 20% ee s = 2</p>	<p>L8: (R,R)-Et-BPE 1a 86% yield, 3% ee cis-3a 6% yield, 30% ee s = 2</p>
<p>L9: (R,R)-Ph-BPE 1a 74% yield, 16% ee cis-3a 18% yield, 79% ee s = 10</p>	

^{a)} Conditions: *rac*-1a (0.2 mmol), CuTC (1 mol%), L* (1.2 mol%), TMDS (0.5 eq) in dry THF (1.0 mL) at room temperature. Acetylation conditions: DMAP (10 mol%), Ac₂O (1.5 eq), and Et₃N (2.5 eq) in DCM (2.0 mL), room temperature, 0.5 h. ^{b)} Yield was determined by ¹⁹F NMR spectroscopy of the crude mixture using PhCF₃ as the internal standard. ^{c)} ee was determined by HPLC analysis. ^{d)} Selectivity factors *s*, *s* = ln[(1 - C)(1 - ee_{sub})]/ln[(1 - C)(1 + ee_{sub})], C = (ee_{sub})/(ee_{sub} + ee_{pro}). The dr values of 3a were all >20:1 as detected by ¹⁹F NMR spectroscopy. CuTC = copper (I) thiophene-2-carboxylate; TMDS, 1,1,3,3-tetramethyldisiloxane.

diastereoselectivity results from the hydride delivery on the less hindered face.^[30,33,38]

We proceeded to an extensive ligand screening (see Section 4.2 in the Supporting Information), the more salient findings of which we outline herein. Biaryl ligand (*R*)-DTBM-SEGPHOS (**L2**), which has frequently been employed in highly enantioselective chiral copper-catalyzed reductions of ketones and imines,^[56–59] was examined, but it gave low conversion (4% yield of *cis*-3a) and low enantioselectivity (17% ee of *cis*-3a). The use of the electron-deficient biaryl ligand (*R*)-difluorophos (**L3**) provided *cis*-3a with a better 76% ee, albeit still with low conversion (13%). Other diphosphine ligands (**L4**–**L7**) bearing various chiral backbones were also evaluated, but they facilitated reductions that resulted in low enantioselectivity and yields or even gave no reaction. Gratifyingly, when (*R,R*)-Ph-BPE (**L9**) was examined, the *N*-protected aziridine 3a was obtained with a promising 79% ee,

Table 2: Selected optimization examples.^{a)}

<p>Ar = </p>		1. CuTC (5 mol%) L9 (6 mol%) Reductant DCM (0.2 M), rt / -65 °C, t		2. DMAP (10 mol%) Ac ₂ O (1.5 eq) DCM (0.1 M), rt, 0.5 h					
Entry	Reductant (ratio to 1a)	t/h	1a ^{b,c}		<i>cis</i> - 3a ^{b,c}		C (%)	<i>S</i> ^d	
			Yield (%)	ee (%)	Yield (%)	ee (%)			
1 ^e	TMDS (0.5)	13	74	16	18	79	17	10	
2	PhSiH ₃ (0.5)	17	60	53	40	91	37	36	
3	PhSiH ₃ (0.5)	20	25	99	75	36	73	9	
4 ^f	(EtO) ₃ SiH (0.5)	72	-	-	n.r.	-	0	-	
5	DMMS (0.5)	-	-	-	trace	-	0	-	
6	HBPIn (0.5)	24	66	38	30	92	29	35	
7	HBPIn (0.65)	24	51	70	48	88	44	33	
8	HBPIn (0.7)	24	40	97	55	79	55	35	
9 ^g	HBPIn (0.65)	36	49	83	51	88	49	41	

^{a)} Conditions: *rac*-1a (0.2 mmol), CuTC (5 mol%), L9 (6 mol%), reducing reagent in dry DCM (1.0 mL) at –60 °C. Acetylation conditions: DMAP (10 mol%), Ac₂O (1.5 eq) and Et₃N (2.5 eq) in DCM (2.0 mL), room temperature, 0.5 h. ^{b)} Yield was determined by ¹⁹F NMR spectroscopy of the crude mixture using PhCF₃ as the internal standard. ^{c)} ee was determined by HPLC analysis. ^{d)} Selectivity factors *s*, *s* = ln[(1 - C)(1 - ee_{sub})]/ln[(1 - C)(1 + ee_{sub})], C = (ee_{sub})/(ee_{sub} + ee_{pro}). The dr values of 3a were all >20:1 as detected by ¹⁹F NMR spectroscopy. ^{e)} CuTC (1 mol%), L1 (1.2 mol%), dry THF (1.0 mL) at room temperature instead. ^{f)} No reaction. ^{g)} 0.3 mmol scale, –65 °C, no acetylation step, isolated yields of 1a and *cis*-N-H-2a.

while the use of the more electron-donating and less bulky (*R,R*)-Et-BPE (**L8**) led only to 30% ee for *cis*-3a.

With the optimal ligand **L9** in hand, further screening found that a dramatic improvement in enantioselectivity (91% ee of *cis*-3a Table 2, entry 2) could be achieved by switching the solvent from THF to dichloromethane (see the complete solvent screening studies in Section 4.3 in the Supporting Information), as well as decreasing the reaction temperature to –60 °C. At this low temperature, the use of more reactive hydride donors such as PhSiH₃ ensured an acceptable turnover.^[60] Under these conditions, the formation of ring-opened product 4a was also suppressed. As previously noted, 2*H*-azirines are very reactive electrophiles: even at low temperatures, the reduction rates for (*R*)- or (*S*)-1a are still very similar, and the control over the conversion needs to be enforced also by the reductant stoichiometry. Limiting the amount of PhSiH₃ used (0.5 equiv., 17 h) led

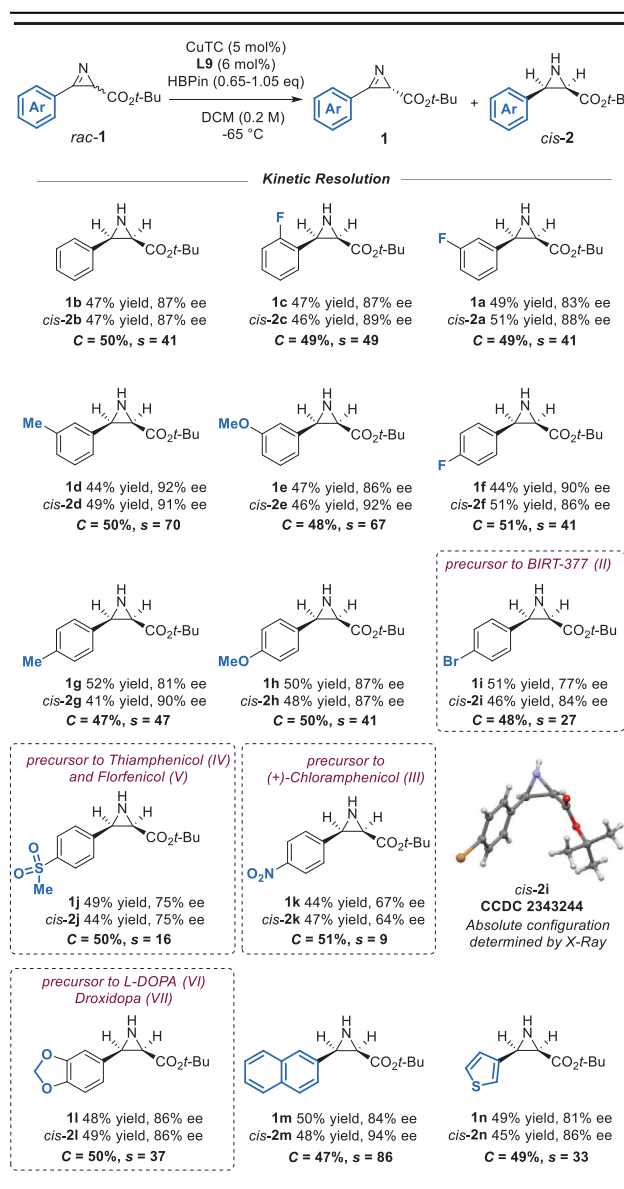
to a 37% conversion of *rac*-**1a**, and thus, the remaining **1a** was recovered with only 53% ee (Table 2, entry 2). However, when we extended the reaction time to 20 h, over-reduction occurred (36% ee and 75% yield for *cis*-**3a**, 99% ee and 25% yield for **1a** Table 2, entry 3). This is likely to be because PhSiH_3 can, in principle, donate three hydrides successively and at different rates.

We therefore screened monohydric sources. $(\text{EtO})_3\text{SiH}$ and dimethoxymethylsilane (DMMS) were found to be too inert under the cryogenic reaction environment (Table 2, entry 4–5). Pinacolborane (HBPin) turned out to be an ideal alternative (Table 2, entry 6–8): an experimentally determined 0.65 equivalents achieved the most effective kinetic resolution in terms of yield and enantioselectivity for both **1a** and *cis*-**3a** (Table 2, entry 7). We moved forward with HBPin as the optimal reductant and determined that -65°C is the ideal temperature for this kinetic resolution (full temperature optimization in Section 4.5 of Supporting Information). With these optimized conditions, *cis*-*N*-H-**2a** was isolated in 51% yield and 88% ee, while **1a** was recovered in 49% yield and 83% ee ($s = 41$) (Table 2, entry 9).

Substrate Scope

Having identified the conditions for the catalytic system, we studied how the variation of the electronic and local steric profile of the aryl group would influence the kinetic resolution process (Table 3). Racemic 2*H*-azirines (**1a**, **1b** and **1d**–**1k**) representing substrates of the classic “Hammett study” type, which are mono-substituted at the *meta*- or *para*- positions, were examined. We found that the presence and position of a fluorine atom on the arene (**1a**, **1f**) with respect to the parent pheny group (**1b**) exerted only a small influence on the reaction outcome, where **1a**, **1b**, and **1f** were all reduced with the same selectivity factor ($s = 41$). On the other hand, the reduction of *ortho*-fluorinated **1c** led to *cis*-**2c** with a marginally increased ee of 89% and a higher s factor of 49. This might be attributed to the steric profile of the *ortho*-fluorine atom. In contrast, the enantioselectivity of the reductions was dramatically improved for 2*H*-azirines that possessed electron-donating groups (EDGs) on the arene (*meta*:- **1d**–**1e**, *para*:- **1g**–**1h**): the asymmetric reduction of *meta*-Me- and MeO-substituted azirines generated reduced products **2d** and **2e** in excellent yields (46%–49%) and with good ee values (91%–92%). Moreover, the unreacted **1d** and **1e** were recovered in equally excellent yields (44%–47%) and enantioselectivity (86%–92%). Reactions proceed efficiently with moderate to highly electron-deficient azirines (*p*-Br, *p*-SO₂Me, *p*-NO₂) to provide free aziridines (**2i**–**2k**) in 44%–47% yield and moderate ee's (67%–77%). The absolute configuration of the *cis*-*N*-H aziridine (**2i**) was determined by X-ray crystallography to be (*R,R*)-**2i**.^[61] By analogy, the same stereochemistry was assigned to the other reduction products. Whereas 2*H*-azirines bearing *para*-substituted electron-donating substituents on the aryl ring (**1g**–**1h**) underwent more enantio-discriminating reductions, those bearing electron-withdrawing groups on *para*-positions were reduced to give products with lower ee. The more

Table 3: Scope of aryl substituents.^{a,b)}

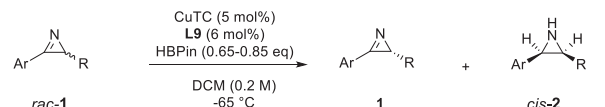
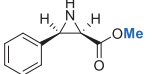
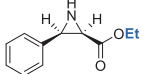
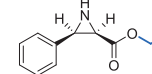
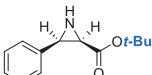
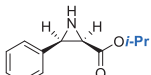
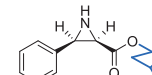
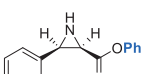
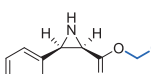
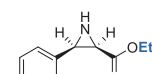
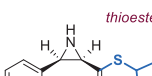
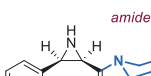
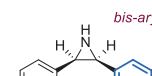


^{a)} Conditions: *rac*-**1** (0.3 mmol), CuTC (5 mol%), **L9** (6 mol%), HBPin (0.65–1.05 eq) in DCM (1.5 mL), -65°C , Ar, 36–45 h. ^{b)} Isolated yield; ee was determined using HPLC analysis on a chiral stationary phase; Selectivity factors $s = \ln[(1-C)(1-ee_{\text{sub}})]/\ln[(1-C)(1+ee_{\text{sub}})]$, $C = (ee_{\text{sub}})/(ee_{\text{sub}} + ee_{\text{pro}})$; The dr values of **2** were all > 20:1 as determined by ¹H NMR spectroscopy.

electron-withdrawing the substituents ($\text{NO}_2 > \text{SO}_2\text{Me} > \text{Br}$), the greater decrease in enantioselectivity. Azirine **1l** bearing an acid labile acetal was reduced to *cis*-**2l**, a valuable optically enriched intermediate for the preparation of prodrugs L-DOPA (VI) and droxidopa (VII), in 86% ee (Scheme 1b). In addition, naphthyl- and thiophene groups were also well-tolerated, providing the corresponding *cis*-**2m** with excellent chiral induction (94% ee, $s = 86$), and *cis*-**2n** with slightly diminished enantioselectivity (86% ee, $s = 33$).

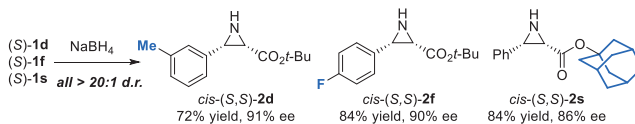
Variations at the ester group of 3-phenyl-2*H*-azirine-2-carboxylates (**1b**, **1o**–**v**) were also surveyed under the optimal

Table 4: Variation of R.^{a,b}

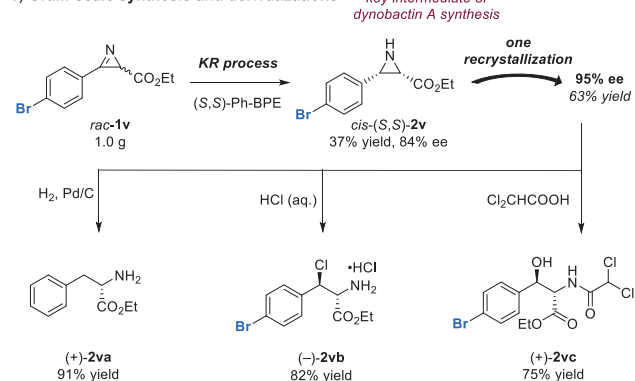
		
Kinetic Resolution		
 1o 45% yield, 82% ee <i>cis</i> - 2o 49% yield, 84% ee C = 49%, s = 29	 1p 47% yield, 77% ee <i>cis</i> - 2p 44% yield, 89% ee C = 46%, s = 40	 1q 47% yield, 89% ee <i>cis</i> - 2q 48% yield, 84% ee C = 51%, s = 34
 1b 47% yield, 87% ee <i>cis</i> - 2b 47% yield, 87% ee C = 50%, s = 41	 1r 47% yield, 89% ee <i>cis</i> - 2r 47% yield, 89% ee C = 50%, s = 51	 1s 44% yield, 88% ee <i>cis</i> - 2s 45% yield, 90% ee C = 49%, s = 55
 1t 46% yield, 88% ee <i>cis</i> - 2t 52% yield, 81% ee C = 52%, s = 27	 1u 44% yield, 89% ee <i>cis</i> - 2u 51% yield, 78% ee C = 53%, s = 24	 1v 54% yield, 60% ee <i>cis</i> - 2v 39% yield, 85% ee C = 41%, s = 23
 1w 50% yield, 72% ee <i>cis</i> - 2w 45% yield, 83% ee C = 46%, s = 23	 1x ^c 51% yield, 86% ee <i>cis</i> - 2x ^c 25% yield, 82% ee C = 51%, s = 28	 1y 49% yield, 63% ee <i>cis</i> - 2y 41% yield, 82% ee C = 43%, s = 19

^a) Conditions: *rac*-**1** (0.3 mmol), CuTC (5 mol%), **L9** (6 mol%), HBPIn (0.65–0.85 eq) in DCM (1.5 mL), –65°C, Ar, 36–45 h. ^b) Yield of the isolated product; ee was determined using HPLC analysis on a chiral stationary phase; selectivity factors *s*, *s* = ln[(1 – C)(1 – ee_{sub})]/ln[(1 – C)(1 + ee_{sub})], C = (ee_{sub})/(ee_{sub} + ee_{pro}). The dr values of **2** were all > 20:1 as determined by ¹H NMR spectroscopy. ^c) *rac*-**1x** (0.1 mmol), HBPIn (1.40 eq), –40°C, 45 h.

KR conditions (Table 4). All of the aziridine carboxylates, including methyl (**2o**), ethyl (**2p**), benzyl (**2q**), *t*-butyl (**2b**), *i*-propyl (**2r**), phenyl (**1t**), 2,2,2-trichloroethyl (**2u**), were satisfactorily obtained in 44%–52% yields and 78%–89% ee. The bulky aziridine adamantyl ester **1s** was reduced to afford *cis*-**2s** in 90% ee with an *s* factor of 55. Aziridine *cis*-**2v** was obtained in good yield and ee. We extended the substrate scope to thioester **1w**, which was reduced to aziridine *cis*-**2w** in excellent yield and moderate enantioselectivity without poisoning the copper catalyst. Reduction of tertiary morpholine amide **1x** was possible under the typical conditions, but the reaction proceeded sluggishly: after 41 h, only 14% conversion was observed (13% yield, 96% ee) (see Supporting Information Section 6.2). When the reaction temperature was raised to –40°C, the conversion reached 51% after 45 h, yielding products **2x** and **1x** with 82% ee and 86% ee, respectively. Finally, we also examined unsymmetrical bis-arylated **1y** as a substrate devoid of any carbonyl group. In the event, its

a) Access to the (S,S)-enantiomers by NaBH₄ reduction

b) Gram-scale synthesis and derivatizations



Scheme 4. a) KR permits the synthesis of both the enantiomers of a given substrate, as exemplified by the preparation of (S,S)-**2d**, (S,S)-**2f** and (S,S)-**2s**. b) Gram-scale KR of *rac*-**1v** to *cis*-(S,S)-**2v** and recrystallization. This aziridine could be transformed to ring-opened derivatives via single operations.

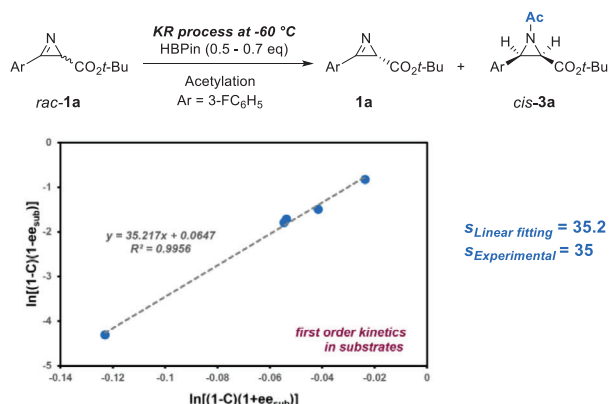
asymmetric reduction also proceeded to provide aziridine *cis*-**2y** in 41% yield and 82% ee.

Derivatization

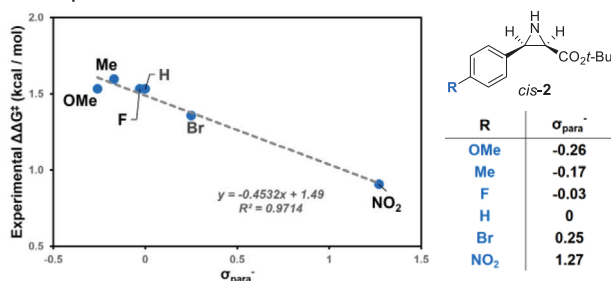
The main advantage of the reductive KR process is that the use of a single chiral catalyst provides access to both enantiomers of the product.^[62–70] As the diastereoselective reduction of 2*H*-azirine-2-carboxylate with NaBH₄ is well documented,^[64] the reduction of enantiomerically enriched azirines (S)-**1d**, (S)-**1f** and (S)-**1s** was carried out to showcase that *cis*-(S,S)-**2d**, (S,S)-**2f** and (S,S)-**2s** can also be obtained in a straightforward manner and with excellent diastereoselectivities (> 20:1 d.r., Scheme 4a).

The robustness of this KR process was demonstrated on a gram-scale kinetic resolution of racemic arylaziridine **1v** using *ent*-**L9** ((S,S)-Ph-BPE) as ligand, by which *cis*-(S,S)-**2v** was delivered in 37% yield and 84% ee. This is the key building block used in the total synthesis of dynobactin A (IX),^[13] which was obtained with comparable yield and ee for the total synthesis (cf. 82% yield over two steps, 87% ee).^[13] (Scheme 4b). Notably, the ee of the 2*H*-azirine-2-carboxylates aziridines can be increased by recrystallization: *cis*-**2v** was enriched to 95% ee after one recrystallization (63% yield). Analogously, one-time recrystallizations of aziridines **2i** (84% ee) and **2w** (83% ee) obtained from KR also led to significantly enhanced enantiomeric excesses (**2i**: > 99.5% ee, 59% yield, **2w**: 98% ee, 69% yield).

The derivatizations of *cis*-*N*-H aziridines have been well-reported.^[8,24,71–77] In our hands, *cis*-(S,S)-**2v** was diastereoselectively transformed into various useful, ring-opened amine

a) Constant s at different conversion points

b) Hammett plot



Scheme 5. a) Experimental conversion and enantioselectivity of *sm* *rac-1a* from the reaction of Table 3 shows first-order kinetics and gives a linear fitting $k_{\text{rel}} = 35.2$ with an $R^2 = 0.996$. b) Correlation between experimentally determined $\Delta\Delta G^\ddagger$ and the σ_{para}^- parameter for *R*.

derivatives by simple operations: hydrogenation provided amino ester **2va** in 91% yield; treatment with HCl delivered ammonium chloride salt **2vb** in 82% yield; ring opening in presence of dichloroacetic acid provided amide **2vc** in 75% yield (Scheme 4b).

Mechanistic Investigations

To gain insight into the reaction mechanism and gain predictive ability for application to desirable new substrates, we used the data in Table 3 for a Hammett plot study. First, we examined whether s was constant and independent of the reaction conversion, which would imply first order in substrate for the selectivity-determining step (Scheme 5a).^[78,79] By linear fitting, we did observe a first-order kinetic profile for the KR of *rac-1a* at -60°C with an $R^2 = 0.996$ and a fitted $s = k_{\text{rel}} = 35.2$.

The s parameter was then expressed as $\Delta\Delta G^\ddagger [-\Delta\Delta G^\ddagger = -RT \ln(s)]$ and plotted against several σ standard parameters. The best correlation was found with σ_{para}^- (Scheme 5b, $y = -0.4532x + 1.49$, $R^2 = 0.971$, refer to the Supporting Information for correlations with other parameters).^[80] Therefore, conjugation effects seem to impact s more than field/inductive effects, with strong electron-withdrawing groups on the arene decreasing the selectivity. The positive sign and small magnitude of the slope value ρ indicates that comparatively

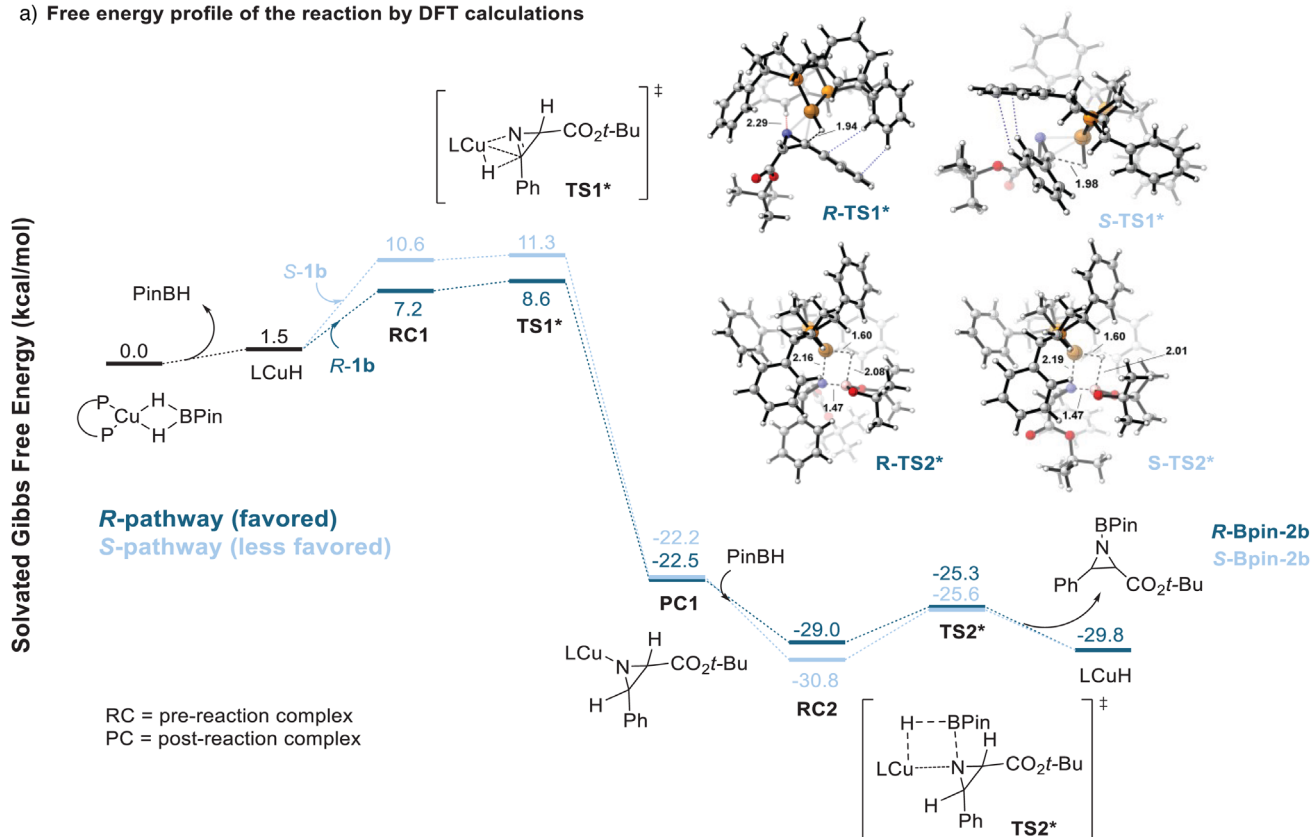
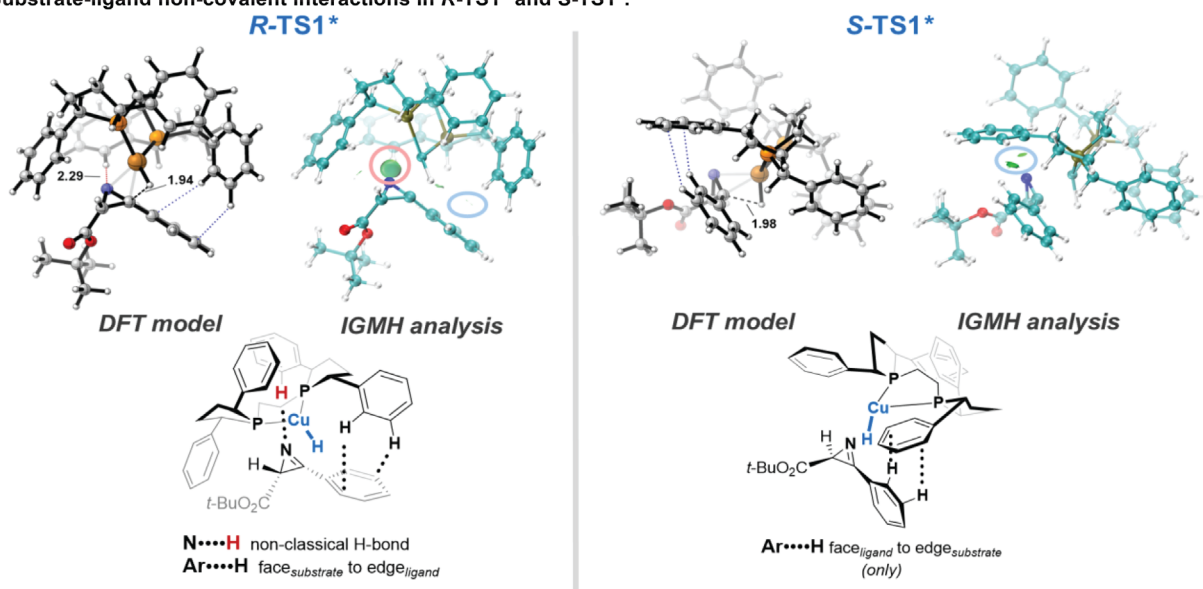
less negative charge is built up at the reaction center in the transition state of the faster-reacting enantiomer.

In our study, the identity of the reductant did not seem to impact the ee,^[81] which, taken together with previous observations for related copper hydride reductions, suggests that the stoichiometric reductant does not participate in the enantioselective step.^[81] On the other hand, over the same 24-h timespan, we observed an increase in conversion with increasing HBPin (see Table 2, Entry 6–8). In line with previous findings,^[60,82] this may indicate that the rate-determining step is the sigma bond metathesis to regenerate the copper hydride species.

To ascertain this, in silico studies of the reaction mechanism of this copper hydride reduction of *2H*-azirines were conducted. density functional theory (DFT) calculations using *rac-1b* as the model substrate and **L9** as the ligand provide the reaction-free energy profile as shown in Scheme 6a. Consistent with the findings by the Hartwig group,^[83] the LCuH-PinBH complex is slightly lower in energy than LCuH by 1.5 kcal mol⁻¹, and is thus the resting state of the catalyst. The reactive LCuH forms upon dissociation and, via a coordinated pre-reaction complex (RC), reduction of azirine **1b** occurs via **TS1*** (barrier of 8.6 and 11.3 kcal mol⁻¹, respectively, for *R-TS1** and *S-TS1**), leading to aziridinyl copper intermediate **PC1** (post-reaction complex). The reduction is highly exergonic, suggesting that this step is irreversible (barrier for reverse pathway ≈ 31 kcal mol⁻¹) and therefore the selectivity-determining step of this reaction. Calculations predicted $\Delta\Delta G^\ddagger = 2.7$ kcal mol⁻¹ between *R-1b* and *S-1b*, in reasonable agreement with experimental result (expt. = 1.5 kcal mol⁻¹, see Section 11.7 in Supporting Information for results with an alternative functional M06). After reduction, complexation of Lewis acidic PinBH to the nucleophilic aziridinyl copper intermediate leads to a more stable intermediate **RC2**, which undergoes a facile metathesis (barrier ≈ 5 kcal mol⁻¹) to regenerate the LCuH catalyst, completing the catalytic cycle. The facile metathesis is attributed to the high nucleophilicity of the aziridinyl copper intermediate. Minimal selectivity between *R-TS2** and *S-TS2** is predicted by calculations, but this is inconsequential, as this is not the selectivity-determining step in this reaction. Overall, the reduction is the rate-determining step of this reaction. Nevertheless, the two barriers **TS1** (7.1 kcal mol⁻¹) and **TS2** (3.7 kcal mol⁻¹) are not very different in energy (only by ~ 3 kcal mol⁻¹), and any change of substrate or reductant could result in a change in the rate-determining step. However, the enantio-determining step will always be the reduction step, due to the high exergonicity and therefore irreversibility associated with this step.

The transition states *R-TS1** and *S-TS1** were further inspected to understand how the observed selectivity is imparted by **L9** (Scheme 6b). Analysis of the more favorable *R-TS1** revealed two non-covalent interactions (NCIs)^[84] between the ligand and the substrate: a non-classical hydrogen bond^[85–87] between a phenyl CH of **L9** and the nitrogen of the azirine substrate, and an edge-to-face aromatic interaction^[88,89] between the phenyl rings on the substrate and ligand **L9**. These interactions were further confirmed by IGMH analysis (independent gradient

a) Free energy profile of the reaction by DFT calculations

b) Substrate-ligand non-covalent interactions in *R*-TS1* and *S*-TS1*.

Scheme 6. a) Free energy profile of the reaction by DFT calculations at B3LYP-D3/def2-TZVPP (IEFPCM, DCM)//B3LYP-D3/def2-SVP (IEFPCM, DCM) level of theory. b) Substrate-ligand non-covalent interactions in *R*-TS1* and *S*-TS1*.

model based on Hirshfeld partition),^[90–93] where attractive interactions between the ligand and substrate (excluding CuH) are revealed as green isosurfaces in Scheme 6b. The larger green isosurface of the non-classical hydrogen bond indicates that it is the dominant interaction, whereas the edge-to-face aromatic interaction is relatively weak and just barely visible at the same isovalue. In contrast, analysis of the

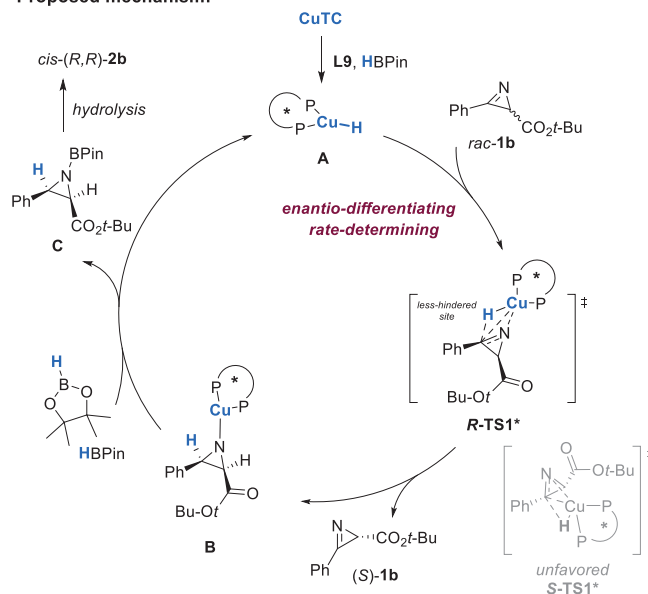
less favorable *S*-TS1* revealed only an edge-to-face aromatic interaction between ligand and substrate, and this was also supported by IGMH analysis. Presumably, *R*-TS1* is favored over *S*-TS1* due to this additional and stronger non-classical hydrogen bond. The critical role of the ligand Ph group, as revealed in these computations, also explains why **L8** Et-BPE is not selective compared to **L9** Ph-BPE (*s* = 2 and 10,

respectively), and also why there is a better selectivity in the reduction of naphthalene substrate **1m** compared to phenyl substrate **1b** ($s = 10$ and 86 , respectively). The absence of non-classical hydrogen bonding in **TS2*** would account for the poor selectivity of the metathesis step, and the potential disruption of these interactions by polar solvent can explain the lower experimentally observed selectivity in THF than in CH_2Cl_2 .

To understand the electronic effect of the aryl group in the Hammett plot study, *R-TS1** and *S-TS1** were located for different R groups at *para*-position of the phenyl ring in **1b**, and $\Delta\Delta G^\ddagger$ between the two TS were calculated (see Table S1 for individual values). The experimental trend was qualitatively reproduced by calculations, showing lower activation energies and earlier transition states on the reaction coordinate for electron-deficient azirines compared to the less reactive electron-rich azirines reacting via later transition states (e.g., $10.0 \text{ kcal mol}^{-1}$ for $\text{R} = \text{OMe}$ vs. $5.1 \text{ kcal mol}^{-1}$ for $\text{R} = \text{NO}_2$, see Figures S9 and S10). However, the electronic effects of the R group on ee did not correlate with the differences in reactivity of the azirines or whether the transition states were early or late.^[94] We attribute the higher selectivity observed in the reactions of azirines bearing more electron-rich substituents to stronger non-classical N-H hydrogen bonding that stabilizes *R-TS1**. Synergistically, the electron-rich Ar on the azirine enhanced the edge-to-face aromatic interaction in *R-TS1** (where Ar offers the face), but weaken the same interaction in *S-TS1** (where Ar acts as the edge),^[89] resulting in further selectivity for *R-TS1**. This hypothesis is supported by slightly shorter N-H hydrogen bond distances and slightly larger isosurfaces for the edge-to-face interaction in *R-TS1** compared to electron-poor substrates (see Table S2, Figures S14–S16). It is likely that substituent effects contribute to the observed electronic effects on selectivity via both of these interactions. Finally, the ester group was not involved in any non-covalent bond interactions in the transition states, implying that it does not play a substantive role in the enantioselectivity of this reaction. This is confirmed experimentally by the comparable selectivity obtained for bis-aryl substrate **1y** without the ester group ($s = 19$ for **1y** vs. **1b**), for which DFT calculations also predicted a similar selectivity ($\Delta\Delta G^\ddagger = 2.4 \text{ kcal mol}^{-1}$ for **1y** vs. $2.7 \text{ kcal mol}^{-1}$ for **1b**).

Based on these results, a full catalytic cycle is proposed in Scheme 7. During the irreversible enantio-discriminating step, the chiral copper hydride complex **A**, formed from precatalyst CuTC-L9 and HBPIn, associates with both enantiomers of **1b** to react via two diastereomeric transition state structures (*R-TS1** and *S-TS1**). Subsequently, species **B** undergoes a sigma bond metathesis with HBPIn to regenerate **A**, and the aziridine exits the cycle as a BPin adduct **C**. According to the results of DFT calculations (Scheme 6a), the rate-determining step in the reaction of **1b** is the reduction (**A** to **B**). Although the rate-determining step could switch to the metathesis step (**B** to **C**) for other substrates and reductants due to the similar barriers for the two steps, the reduction step (**A** to **B**) remains irreversible and enantio-determining due to the high exergonicity associated with the hydride addition. Upon quenching, **C** provides the aziridine-2-carboxylate product **2b**.

Proposed mechanism:



Scheme 7. Proposed reaction mechanism for the KR of 2H-azirines.

Conclusion

We have reported the first copper hydride catalyzed kinetic resolution of 2H-azirines. A series of 3-aryl-2H-azirine-2-carboxylates are prepared in high diastereo- and enantioselectivity. These enantiomerically enriched N-H aziridines are versatile synthetic intermediates that can be used in many synthetic applications. We have demonstrated a gram-scale synthesis that provides a key intermediate in the total synthesis of dynobactin A. We highlight the advantages of the KR process that allows access to both enantiomers of the 2H-azirine-2-carboxylates. A linear free-energy relationship between $\Delta\Delta G^\ddagger$ and σ_{para}^- was identified. The DFT calculations shed light on the origin of the enantioselectivity of the reaction, where two NCIs (non-classical H-bonding and edge-to-face aromatic interactions) play synergistic roles in the transition state that leads to the observed selectivity.

Supporting Information

The supplemental figures, experimental procedures and characterization data that support this study are available in the supplementary material of this article.

Acknowledgements

The financial support of a General Research Fund from the Research Grants Council of Hong Kong (HKU 17312222), The State Key Laboratory of Synthetic Chemistry and the Laboratory for Synthetic Chemistry and Chemical Biology under the Health@InnoHK Program launched by Innovation and Technology Commission, The Government of Hong Kong Special Administrative Region of the People's Republic of China.

Conflict of Interests

The authors declare no conflict of interest.

Data Availability Statement

The data that support the findings of this study are available in the supplementary material of this article.

Keywords: Asymmetric catalysis • Aziridines • Azirines • Copper • Kinetic resolution

- [1] H. J. Ha, J. H. Jung, W. K. Lee, *Asian J. Org. Chem.* **2014**, *3*, 1020–1035.
- [2] W. K. Lee, H.-J. Ha, *Aldrichimica. Acta.* **2003**, *36*, 57–63.
- [3] L. Huang, W. Zhao, R. J. Staples, W. D. Wulff, *Chem. Sci.* **2013**, *4*, 622–628.
- [4] Y. Shishido, F. Ito, H. Morita, M. Ikonaka, *Bioorg. Med. Chem. Lett.* **2007**, *17*, 6887–6890.
- [5] B. Degel, P. Staib, S. Rohrer, J. Scheiber, E. Martina, C. Büchold, K. Baumann, J. Morschhäuser, T. Schirmeister, *ChemMedChem* **2008**, *3*, 302–315.
- [6] C. Büchold, Y. Hemberger, C. Heindl, A. Welker, B. Degel, T. Pfeuffer, P. Staib, S. Schneider, P. J. Rosenthal, J. Gut, *ChemMedChem* **2011**, *6*, 141–152.
- [7] A. P. Patwardhan, V. R. Pulgam, Y. Zhang, W. D. Wulff, *Angew. Chem., Int. Ed.* **2005**, *44*, 6169–6172.
- [8] S. P. Bew, J. Liddle, D. L. Hughes, P. Pesce, S. M. Thurston, *Angew. Chem., Int. Ed.* **2017**, *56*, 5322–5326.
- [9] F. A. Davis, P. Zhou, *Tetrahedron Lett.* **1994**, *35*, 7525–7528.
- [10] Z. Wang, F. Li, L. Zhao, Q. He, F. Chen, C. Zheng, *Tetrahedron* **2011**, *67*, 9199–9203.
- [11] J. C. Antilla, W. D. Wulff, *Angew. Chem., Int. Ed.* **2000**, *39*, 4518–4521.
- [12] M. Rajappa, (P. E. Limited), WO2016147132A1, **2016**.
- [13] F. Schneider, Y. Guo, Y.-C. Lin, K. J. Eberle, D. Chiodi, J. A. Greene, C. Lu, P. S. Baran, *J. Am. Chem. Soc.* **2023**, *146*, 6444–6448.
- [14] T. M. Solá, I. Churcher, W. Lewis, R. A. Stockman, *Org. Biomol. Chem.* **2011**, *9*, 5034–5035.
- [15] I. Khantikaew, M. Takahashi, T. Kumamoto, N. Suzuki, T. Ishikawa, *Tetrahedron* **2012**, *68*, 878–882.
- [16] P. V. Kattamuri, Y. Xiong, Y. Pan, G. Li, *Org. Biomol. Chem.* **2013**, *11*, 3400–3408.
- [17] T. Hashimoto, H. Nakatsu, K. Yamamoto, S. Watanabe, K. Maruoka, *Chem. Asian J.* **2011**, *6*, 607–613.
- [18] T. Haga, T. Ishikawa, *Tetrahedron* **2005**, *61*, 2857–2869.
- [19] S. G. Davies, A. M. Fletcher, A. B. Frost, J. A. Lee, P. M. Roberts, J. E. Thomson, *Tetrahedron* **2013**, *69*, 8885–8898.
- [20] F. Colpaert, S. Mangelinckx, S. De Brabandere, N. De Kimpe, *J. Org. Chem.* **2011**, *76*, 2204–2213.
- [21] J. Egloff, M. Ranocchiari, A. Schira, C. Schotes, A. Mezzetti, *Organometallics* **2013**, *32*, 4690–4701.
- [22] Y. Zhang, Z. Lu, A. Desai, W. D. Wulff, *Org. Lett.* **2008**, *10*, 5429–5432.
- [23] Y. Zhang, A. Desai, Z. Lu, G. Hu, Z. Ding, W. D. Wulff, *Chem. - Eur. J.* **2008**, *14*, 3785–3803.
- [24] Z. Lu, Y. Zhang, W. D. Wulff, *J. Am. Chem. Soc.* **2007**, *129*, 7185–7194.
- [25] A. A. Desai, R. Morán-Ramallal, W. D. Wulff, *Org. Synth.* **2003**, *88*, 224–238.
- [26] H. Heimgartner, *Angew. Chem., Int. Ed.* **1991**, *30*, 238–264.
- [27] S. Calvo-Losada, J. J. Quirante, D. Suárez, T. L. Sordo, *J. Comput. Chem.* **1998**, *19*, 912–922.
- [28] F. Palacios, A. M. O. de Retana, E. M. de Marigorta, J. M. de los Santos, *Eur. J. Org. Chem.* **2001**, *2001*, 2401–2414.
- [29] Y. Gök, T. Noël, J. Van der Eycken, *Tetrahedron Asymm* **2010**, *21*, 2275–2280.
- [30] D. An, X. Guan, R. Guan, L. Jin, G. Zhang, S. Zhang, *Chem. Commun.* **2016**, *52*, 11211–11214.
- [31] H. Hu, Y. Liu, L. Lin, Y. Zhang, X. Liu, X. Feng, *Angew. Chem., Int. Ed.* **2016**, *55*, 10098–10101.
- [32] S. Nakamura, D. Hayama, *Angew. Chem., Int. Ed.* **2017**, *56*, 8785–8789.
- [33] H. Hu, J. Xu, W. Liu, S. Dong, L. Lin, X. Feng, *Org. Lett.* **2018**, *20*, 5601–5605.
- [34] S. Nakamura, D. Hayama, M. Miura, T. Hatanaka, Y. Funahashi, *Org. Lett.* **2018**, *20*, 856–859.
- [35] Q. Peng, D. Guo, J. Bie, J. Wang, *Angew. Chem., Int. Ed.* **2018**, *57*, 3767–3771.
- [36] H. J. Zhang, Y. C. Xie, L. Yin, *Nat. Commun.* **2019**, *10*, 1699.
- [37] Q. Peng, D. Guo, B. Zhang, L. Liu, J. Wang, *Chem. Commun.* **2020**, *56*, 12427–12430.
- [38] Y.-L. Pan, Y.-B. Shao, J. Wang, Z. Liu, L. Chen, X. Li, *ACS Catal.* **2021**, *11*, 13752–13760.
- [39] Z.-Y. Zhao, M. Cui, E. Irran, M. Oestreich, *Angew. Chem., Int. Ed.* **2022**, *62*, e202215032.
- [40] F. Xie, J. Zhao, D. Ren, J. Xue, J. Wang, Q. Zhao, L. Liu, X. Liu, *Org. Lett.* **2023**, *25*, 8530–8534.
- [41] S. R. Harutyunyan, C. Ni, T. F. Ramspoth, M. C. Reis, *Angew. Chem., Int. Ed.* **2024**, e202415623.
- [42] B. Chen, K. F. Cheng, P. Chiu, *Tetrahedron Lett.* **1998**, *39*, 9229–9232.
- [43] P. Chiu, C.-P. Szeto, Z. Geng, K.-F. Cheng, *Org. Lett.* **2001**, *3*, 1901–1903.
- [44] P. Chiu, S. K. Leung, *Chem. Commun.* **2004**, 2308–2309.
- [45] W. K. Chung, P. Chiu, *Synlett* **2005**, *2005*, 55–58.
- [46] N. Li, J. Ou, M. Miesch, P. Chiu, *Org. Biomol. Chem.* **2011**, *9*, 6143–6147.
- [47] K. C. Wong, E. Ng, W. T. Wong, P. Chiu, *Eur. J. Chem.* **2016**, *22*, 3709–3712.
- [48] E. W. H. Ng, K.-H. Low, P. Chiu, *J. Am. Chem. Soc.* **2018**, *140*, 3537–3541.
- [49] S. Guo, K. C. Wong, S. Scheeff, Z. He, W. T. K. Chan, K.-H. Low, P. Chiu, *J. Org. Chem.* **2021**, *87*, 429–452.
- [50] Y. Shi, J. Wang, Q. Yin, X. Zhang, P. Chiu, *Org. Lett.* **2021**, *23*, 5658–5663.
- [51] V. Jurkauskas, S. L. Buchwald, *J. Am. Chem. Soc.* **2002**, *124*, 2892–2893.
- [52] X. Dong, A. Weickgenannt, M. Oestreich, *Nat. Commun.* **2017**, *8*, 15547.
- [53] S. Lee, D. H. Ryu, J. Yun, *Adv. Synth. Catal.* **2021**, *363*, 2377–2381.
- [54] S. Nakamura, *Chem. Asian J.* **2019**, *14*, 1323–1330.
- [55] P. Roth, P. G. Andersson, P. Somfai, *Chem. Commun.* **2002**, 1752–1753.
- [56] B. H. Lipshutz, A. Lower, K. Noson, *Org. Lett.* **2002**, *4*, 4045–4048.
- [57] B. H. Lipshutz, B. A. Frieman, *Angew. Chem., Int. Ed.* **2005**, *44*, 6345–6348.
- [58] B. H. Lipshutz, A. Lower, R. J. Kucejko, K. Noson, *Org. Lett.* **2006**, *8*, 2969–2972.
- [59] B. H. Lipshutz, H. Shimizu, *Angew. Chem., Int. Ed.* **2004**, *43*, 2228–2230.
- [60] J. S. Bandar, M. T. Pirnot, S. L. Buchwald, *J. Am. Chem. Soc.* **2015**, *137*, 14812–14818.
- [61] Deposition Number(s) **2343244** (for **cis-2i**) contain(s) the supplementary crystallographic data for this paper. These

- data are provided free of charge by the joint Cambridge Crystallographic Data Centre and Fachinformationszentrum Karlsruhe, [Access Structures service](#).
- [62] F. A. Davis, G. V. Reddy, H. Liu, *J. Am. Chem. Soc.* **1995**, *117*, 3651–3652.
- [63] L. Gentilucci, Y. Grijzen, L. Thijs, B. Zwanenburg, *Tetrahedron Lett.* **1995**, *36*, 4665–4668.
- [64] M. M. Verstappen, G. J. Ariaans, B. Zwanenburg, *J. Am. Chem. Soc.* **1996**, *118*, 8491–8492.
- [65] T. Sakai, I. Kawabata, T. Kishimoto, T. Ema, M. Utaka, *J. Org. Chem.* **1997**, *62*, 4906–4907.
- [66] F. A. Davis, H. Liu, C.-H. Liang, G. V. Reddy, Y. Zhang, T. Fang, D. D. Titus, *J. Org. Chem.* **1999**, *64*, 8929–8935.
- [67] S. Sakamoto, T. Inokuma, Y. Takemoto, *Org. Lett.* **2011**, *13*, 6374–6377.
- [68] K. Okamoto, A. Nanya, A. Eguchi, K. Ohe, *Angew. Chem., Int. Ed.* **2018**, *57*, 1039–1043.
- [69] H. Deng, T.-T. Liu, Z.-D. Ding, W.-L. Yang, X. Luo, W.-P. Deng, *Org. Chem. Front.* **2020**, *7*, 3247–3252.
- [70] With the material at hand, we explored the viability of a dynamic kinetic resolution process. Unfortunately, subjecting enantioenriched **1a** to the common bases compatible with copper hydride chemistry at room temperature revealed that no deprotonation and racemization occurred (See Section 7 in Supporting Information).
- [71] T. N. Wade, *J. Org. Chem.* **1980**, *45*, 5328–5333.
- [72] M. A. Letavic, J. T. Barberia, T. J. Carty, J. R. Hardink, J. Liras, L. L. Lopresti-Morrow, P. G. Mitchell, M. C. Noe, L. M. Reeves, S. L. Snow, *Bioorg. Med. Chem. Lett.* **2003**, *13*, 3243–3246.
- [73] N. Inguibert, P. Coric, H. Dhotel, E. Bonnard, C. Llorens-Cortes, N. De Mota, M. C. Fournié-Zaluski, B. P. Roques, *Pept. Res.* **2005**, *65*, 175–188.
- [74] S. P. Bew, R. Carrington, D. L. Hughes, J. Liddle, P. Pesce, *Adv. Synth. Catal.* **2009**, *351*, 2579–2588.
- [75] S. P. Bew, S. A. Fairhurst, D. L. Hughes, L. Legentil, J. Liddle, P. Pesce, S. Nigudkar, M. A. Wilson, *Org. Lett.* **2009**, *11*, 4552–4555.
- [76] W. Zhao, Z. Lu, W. D. Wulff, *J. Org. Chem.* **2014**, *79*, 10068–10080.
- [77] F. Schneider, Y. Guo, Y.-C. Lin, K. Eberle, D. Chiodi, J. Greene, C. Lu, P. Baran, *Chem Rxiv preprint* **2023**, <https://doi.org/10.26434/chemrxiv-2023-kw0xn>.
- [78] D. G. Blackmond, N. S. Hodnett, G. C. Lloyd-Jones, *J. Am. Chem. Soc.* **2006**, *128*, 7450–7451.
- [79] M. D. Greenhalgh, J. E. Taylor, A. D. Smith, *Tetrahedron* **2018**, *74*, 5554–5560.
- [80] C. Hansch, A. Leo, R. Taft, *Chem. Rev.* **1991**, *91*, 165–195.
- [81] B. H. Lipshutz, K. Noson, W. Chrisman, A. Lower, *J. Am. Chem. Soc.* **2003**, *125*, 8779–8789.
- [82] J. T. Issenhuth, F. P. Notter, S. Dagorne, A. Dedieu, S. Bellemin-Laponnaz, *Eur. J. Inorg. Chem.* **2010**, *2010*, 529–541.
- [83] Y. Xi, J. F. Hartwig, *J. Am. Chem. Soc.* **2017**, *139*, 12758–12772.
- [84] A. J. Neel, M. J. Hilton, M. S. Sigman, F. D. Toste, *Nature* **2017**, *543*, 637–646.
- [85] R. C. Johnston, P. H.-Y. Cheong, *Org. Biomol. Chem.* **2013**, *11*, 5057–5064.
- [86] N. V. Belkova, E. S. Shubina, L. M. Epstein, *Acc. Chem. Res.* **2005**, *38*, 624–631.
- [87] I. Alkorta, I. Rozas, J. Elguero, *Chem. Soc. Rev.* **1998**, *27*, 163–170.
- [88] C. A. Hunter, J. K. M. Sanders, *J. Am. Chem. Soc.* **1990**, *112*, 5525–5534.
- [89] S. E. Wheeler, K. N. Houk, *Mol. Phys.* **2009**, *107*, 749–760.
- [90] T. Lu, Q. Chen, *J. Comput. Chem.* **2022**, *43*, 539–555.
- [91] E. R. Johnson, S. Keinan, P. Mori-Sánchez, J. Contreras-García, A. J. Cohen, W. Yang, *J. Am. Chem. Soc.* **2010**, *132*, 6498–6506.
- [92] T. Lu, *J. Chem. Phys.* **2024**, *161*, 082503.
- [93] T. Lu, F. Chen, *J. Comput. Chem.* **2012**, *33*, 580–592.
- [94] The electronic effects of R on the enantioselectivity were estimated to be < 0.05 kcal/mol, and could not account for the 0.62 kcal/mol difference between R = NO₂ and R = H: (see SI-section 11.3 for details).

Manuscript received: December 03, 2024

Revised manuscript received: February 27, 2025

Accepted manuscript online: March 21, 2025

Version of record online: May 28, 2025